九州工業大学学術機関リポジトリ

Kyutacar

Kyushu Institute of Technology Academic Repository

Alternative cyanide-binding modes to the haem iron in haem oxygenase

	Sugishima Masakazu, Oda Kenji, Ogura Takashi, Sakamoto Hiroshi, Noguchia Masato, Fukuyamae Keiichi
journal or publication title	Acta Crystallographica Section F: Structural Biology and Crystallization Communications
volume	63
number	6
page range	471-474
year	2007-06-01
URL	http://hdl.handle.net/10228/00006121

protein structure communications

Alternative cyanide-binding modes to the haem iron in haem oxygenase

Masakazu Sugishima,[a] Kenji Oda,[b] Takashi Ogura,[c] Hiroshi Sakamoto,[d] Masato Noguchi[a] and Keiichi Fukuyama[e,f]*

[a]Department of Medical Biochemistry, Kurume University School of Medicine, Japan, [b]Graduate School of Arts and Science, University of Tokyo, Japan, [c]Department of Life Science, Faculty of Science, University of Hyogo, Japan, [d]Department of Bioscience and Bioinformatics, Faculty of Computer Science and Systems Engineering, Kyushu Institute of Technology, Japan, [e]Department of Biological Sciences, Graduate School of Science, Osaka University, Japan, and [f]RIKEN Harima Institute/SPring-8, Japan

Correspondence e-mail:
fukuyama@bio.sci.osaka-u.ac.jp

Cyanide is a well known potent inhibitor of haem proteins, including haem oxygenase (HO). Generally, cyanide coordinates to the ferric haem iron with a linear binding geometry; the $Fe-C-N$ angle ranges from 160 to 180°. The $Fe-C-N$ angle observed in the crystal structure of haem–HO bound to cyanide prepared at alkaline pH was 166°. Here, it is reported that cyanide can bind to the haem iron in HO in a bent mode when the ternary complex is prepared at neutral pH; a crystal structure showed that the $Fe-C-N$ angle was bent by 47°. Unlike the ternary complex prepared at alkaline pH, in which the haem group, including the proximal ligand and the distal helix, was displaced upon cyanide binding, the positions of the haem group and the distal helix in the complex prepared at neutral pH were nearly identical to those in haem–HO. Cyanide that was bound to haem–HO with a bent geometry was readily photodissociated, whereas that bound with a linear geometry was not photodissociated. Thus, alternative cyanide-binding modes with linear and bent geometries exist in the crystalline state of haem–HO.

1. Introduction

Cyanide binds tightly to the ferric haem iron and inhibits the binding of intrinsic ligands to the haem iron of a given haem protein: *e.g.* of molecular oxygen to the haem iron in haem proteins such as cytochrome *c* oxidase. It is known from the crystal structures and spectroscopic and theoretical studies of several haem proteins that the coordination of cyanide to the ferric haem iron at the distal site is stabilized by the linear binding geometry; the $Fe-C-N$ angle is between 160 and 180° (Bolognesi *et al.*, 1999; Nardini *et al.*, 1995), which is similar to the binding of CO to the ferrous haem iron, whereas O_2 or NO binds to the haem iron with a bent geometry (the $Fe-O-O$ angle is less than 140°). Of the 43 crystal structures of cyanide-bound haem proteins at resolutions higher than 2.0 Å that have been deposited in the Protein Data Bank, seven crystal structures showed unusual bending angles in the haem–cyanide binding mode (Bolognesi *et al.*, 1999; Nardini *et al.*, 1995; Blair-Johnson *et al.*, 2001; Sjögren & Hajdu, 2001; Fedorov *et al.*, 2003; Evans *et al.*, 1994; Neya *et al.*, 1993; Sen *et al.*, 2004). The orientations of the diatomic ligands determined by X-ray crystallography, however, remain ambiguous owing to the limited resolutions and the anisotropic thermal vibration of haem and its ligands (Stec & Phillips, 2001).

Here, we report a new cyanide-binding mode in rat haem oxygenase (HO) that differs from that observed previously in HO bound to haem and CN^- (CN^-–haem–HO) prepared at alkaline pH (Sugishima *et al.*, 2003). HO is an enzyme that catalyzes the cleavage of haem by using O_2 and reducing equivalents to produce biliverdin IXα, iron and CO (Tenhunen *et al.*, 1968). The effect of diatomic ligand (X–Y) binding on the conformation of the haem pocket in HO in complex with haem (haem–HO) differs depending on the bending angle of the ligand (Sugishima *et al.*, 2003); when the $Fe-X-Y$ angle is close to linear, the haem is shifted together with the proximal ligand towards the inside of HO and the distal helix is shifted in the opposite direction, which is accompanied by movement of a nearby helix and

protein structure communications

	CN⁻–haem–HO (pH 6.8)	Photolysis of CN⁻–haem–HO (pH 6.8)		Photolysis of CN⁻–haem–HO (pH 9.7)	
		In the dark	Laser on	In the dark	Laser on
Diffraction statistics					
Unit-cell parameters (Å)	$a = 65.38$, $c = 121.03$	$a = 65.11$, $c = 120.33$		$a = 65.34$, $c = 120.40$	
Space group	$P3_221$				
Resolution range (Å)	50.0–1.85 (1.92–1.85)	20.0–2.0 (2.07–2.00)		20.0–2.0 (2.07–2.00)	
No. of observations	215344	108693	107876	97643	92256
No. of unique reflections	25213	19018	19152	18922	18744
Redundancy	8.5	5.7	5.6	5.2	4.9
Completeness (%)	95.7 (89.3)	92.3 (87.2)	92.8 (92.2)	91.1 (86.9)	90.2 (84.3)
Mean $I/\sigma(I)$	15.6 (5.8)	13.8 (3.5)	13.4 (3.4)	15.3 (3.7)	17.4 (3.8)
R_{sym}†	0.046 (0.335)	0.080 (0.423)	0.083 (0.417)	0.060 (0.400)	0.061 (0.420)
Refinement statistics					
R/R_{free}‡	0.194/0.218	0.210/0.224	0.208/0.225	0.215/0.252	0.214/0.245
R.m.s. deviations from ideality					
Bond lengths (Å)	0.006	0.007	0.007	0.007	0.007
Angles (°)	1.138	1.132	1.117	1.149	1.156

† $R_{sym} = \sum_{hkl} \sum_i |I_i(hkl) - \langle I(hkl)\rangle| / \sum_{hkl} \sum_i I_i(hkl)$, where $\langle I(hkl)\rangle$ is the mean intensity for multiple recorded reflections. ‡ $R = \sum |F_{obs}(hkl) - F_{calc}(hkl)| / \sum |F_{obs}(hkl)|$. R_{free} is the R value calculated for 10% of the data set not included in the refinement.

breakdown of one of the salt bridges stabilizing the haem binding to HO, whereas large structural changes did not occur when the Fe—X—Y bond is severely bent. It is likely that such a conformational change occurs to avoid steric hindrance between the distal ligand and the distal helix. Thus, the linear or bent binding of the diatomic ligand to the haem iron can be validated for HO based on the conformation of haem pocket, even if the resolution of the X-ray analysis is approximately 2.0 Å.

2. Experimental

CN⁻–haem–HO was prepared and crystallized as described elsewhere (Sugishima *et al.*, 2003). CN⁻–haem–HO crystals were prepared at several pH values by soaking cocrystallized CN⁻–haem–HO for a few minutes in each of the following solutions: 5 m*M* KCN, crystallization solution (4 *M* sodium formate and 50 m*M* potassium phosphate pH 6.8) containing 5 m*M* potassium cyanide; 10 m*M* KCN, crystallization solution containing 10 m*M* potassium cyanide; 20 m*M*

KCN, crystallization solution containing 20 m*M* potassium cyanide; 40 m*M* KCN, crystallization solution containing 40 m*M* potassium cyanide; 50 m*M* KCN, crystallization solution containing 50 m*M* potassium cyanide; 5 m*M* KCN pH 9.7, crystallization solution containing 5 m*M* potassium cyanide in which potassium phosphate was replaced with sodium borate pH 9.7. Each crystal was isomorphous to the previously reported crystal of CN⁻–haem–HO (50 m*M* KCN pH 9.7). Diffraction data for the CN⁻–haem–HO crystals obtained at several pH values were collected using synchrotron radiation ($\lambda = 0.750$ Å) at 100 K at the BL41XU beamline in SPring-8 with a MAR CCD detector. Diffraction data were processed, merged and scaled using the *HKL*-2000 program suite (Otwinowski & Minor, 1997). The refinement of CN⁻–haem–HO pH 6.8 was performed with *CNS* (Brünger *et al.*, 1998) in a similar manner as for the previously reported CN⁻–haem–HO pH 9.7 (Sugishima *et al.*, 2003). Diffraction statistics and refinement statistics are given in Table 1.

Diffraction data for the CN⁻–haem–HO crystals in the dark and under illumination provided by a red laser were collected using synchrotron radiation ($\lambda = 1.000$ Å) and an open-flow helium cryostat
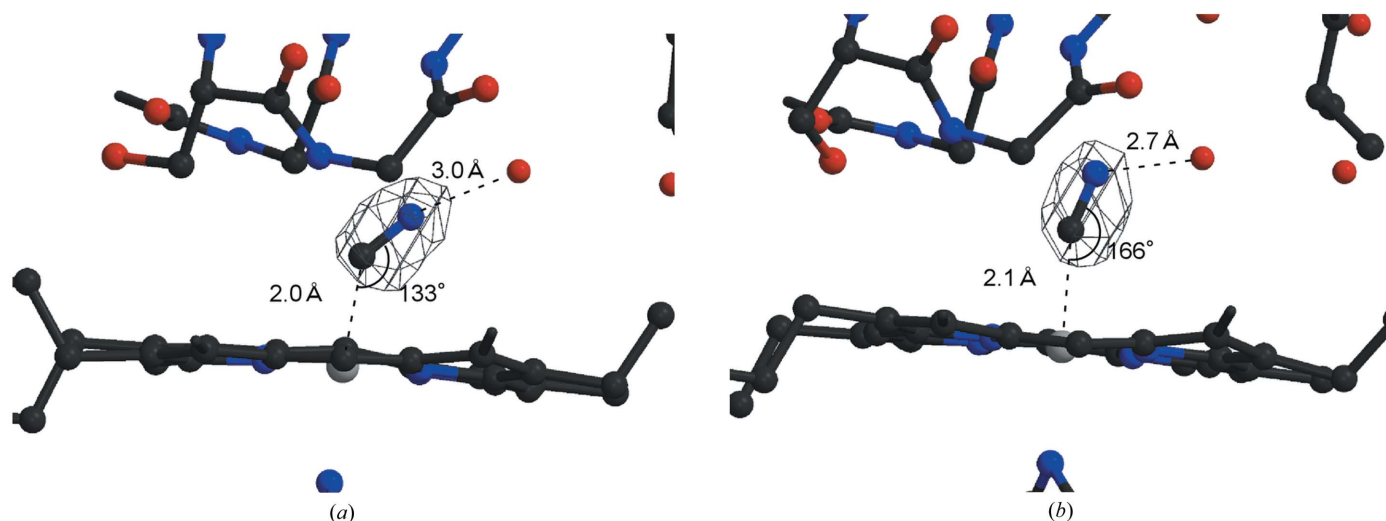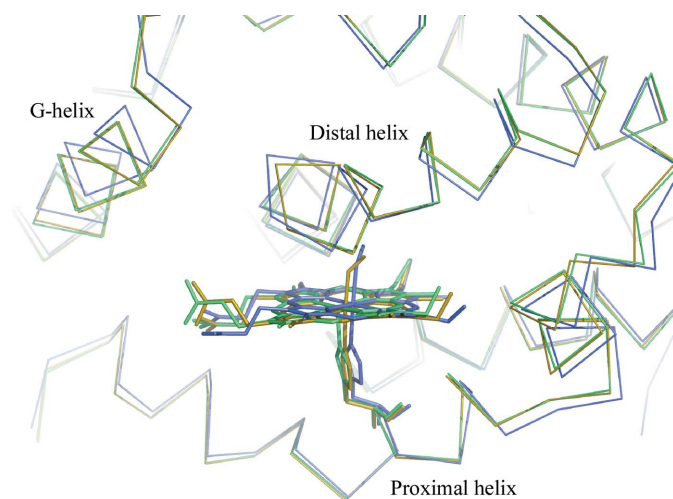

Figure 1
Two different cyanide-binding modes in HO. The $F_o - F_c$ map omitting the distal ligand is superimposed on the ball-and-stick model around the haem group. (*a*) The bent binding mode (5 m*M* KCN pH 6.8). (*b*) The linear binding mode (50 m*M* KCN pH 9.7; Sugishima *et al.*, 2003).

(Nakasako *et al.*, 2002) at ∼35 K at the BL44B2 beamline in SPring-8. Data collection was carried out as for the CO-bound haem–HO complex (CO–haem–HO; Sugishima *et al.*, 2004). For data collection under illumination, the crystal was continuously illuminated for 10 min before and during data collection using a He–Ne laser (15 mW, 632.8 nm; Melles Griot, Irvine, CA, USA). To increase the signal-to-noise ratio of the difference Fourier map, the data sets for CN⁻–haem–HO in the dark and under illumination were collected from the same crystal under the same conditions. Before calculating the difference Fourier maps, the models of CN⁻–haem–HO pH 6.8 and pH 9.7 were independently refined using the diffraction data collected in these experiments individually.
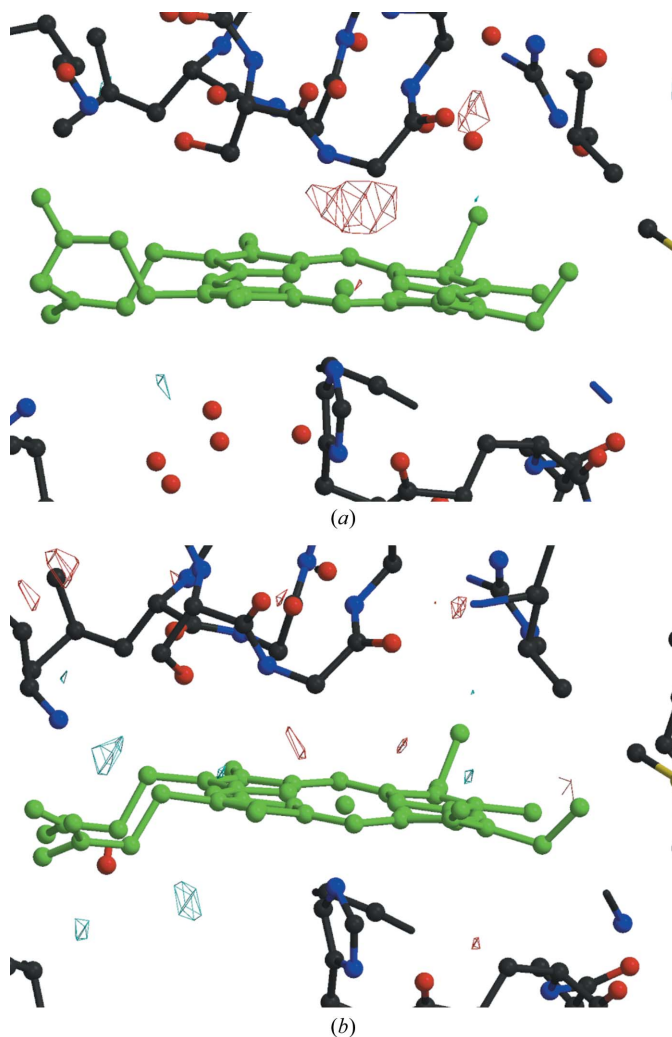
3. Results and discussion

The crystal structure of haem–HO bound to cyanide (CN⁻–haem–HO) was newly determined at neutral pH. Notably, the Fe—C—N angle was bent by 47° (Fig. 1). This binding mode differed from that in the previously determined structure of CN⁻–haem–HO at alkaline pH (Sugishima *et al.*, 2003), in which the Fe—C—N angle was almost linear. We previously reported that upon cyanide binding at alkaline pH, the haem together with the proximal ligand shifted in one direction and the distal helix shifted in the opposite direction, which was accompanied by movement of the G-helix, Lys179 and Arg183 of which are involved in salt bridges to a haem propionate. These movements caused conformational changes of this propionate and the Lys179 side chain and the breakdown of one of the salt bridges (between Lys179 and the propionate). However, none of these conformational changes occurred upon cyanide binding at neutral pH as shown by the present study (Fig. 2); the unusual bending in the Fe—C—N angle did not produce steric hindrance between the distal helix and the cyanide bound to the haem iron. The structure around the haem-binding site in CN⁻–haem–HO at neutral pH is very similar to that in ferric haem–HO at alkaline pH (Sugishima *et al.*, 2000), indicating that the structural changes described above are not a consequence of the pH difference.

A linear Fe–cyanide binding geometry was observed in the ternary complex prepared at a KCN concentration of 20–50 m*M* at pH 7.8–9.7, whereas the bent mode was observed with a KCN concentration of 5–10 m*M* at pH 6.8–7.1 (data not shown). A linear binding geometry was also observed when the pH was changed to alkaline at 5 m*M* KCN. Thus, it is likely that the cyanide-binding mode of haem–HO in the crystalline state depends on the pH.

Interestingly, X-ray diffraction analysis for the CN⁻–haem–HO crystals in the dark and under illumination indicated that cyanide binding in the bent mode was light-sensitive. Difference Fourier maps clearly showed that the cyanide at the distal side of the haem at neutral pH was dissociated from the haem iron by laser irradiation, but did not dissociate at alkaline pH under the same experimental conditions (Fig. 3). The location of the cyanide dissociated from the haem iron at neutral pH was not identified, although CO was trapped in the hydrophobic cavity of the distal haem pocket when the crystal of the CO–haem–HO complex was irradiated under similar conditions (Sugishima *et al.*, 2004). The reason why CN⁻ was not trapped in the hydrophobic cavity may be that CN⁻ has anionic character, unlike CO. The observation of differing light-sensitivities of the Fe—CN⁻ bonds depending on the binding geometry supports the

Figure 2
Superimposition of haem–HO (green; Sugishima *et al.*, 2003), CN⁻–haem–HO (yellow, pH 6.8) and CN⁻–haem–HO (blue, pH 9.7). Except for the proximal histidine, only the Cᵅ traces are shown for clarity. The crystal structures of CN⁻–haem–HO at pH 6.8 and 9.7 were superimposed on the structure of haem–HO so as to minimize the r.m.s. deviations of Cᵅ atoms. Following the distal helix is the G-helix, which contains the basic residues (Lys179 and Arg183) involved in the salt bridges to haem propionates.

Figure 3
Photodissociation of cyanide. A difference Fourier map calculated between data sets obtained in the dark and under continuous illumination from a red laser is superimposed on the ball-and-stick model around the haem group. Blue and red indicate newly appeared and the diminished densities, respectively (contoured at ±3σ). (*a*) 5 m*M* KCN pH 6.8. (*b*) 50 m*M* KCN pH 9.7.

existence of the alternative cyanide-binding modes in the haem–HO crystal.

In the present analysis, we have identified alternative binding modes of cyanide in crystals depending on pH (bent at pH 6.8–7.1, linear at pH 7.8–9.7). The bent binding mode of cyanide observed in the present study may represent a state preceding the previously reported conformational change in the haem pocket that results from cyanide binding with a linear binding mode (Sugishima *et al.*, 2003). It is uncertain at present why the cyanide-binding mode in the crystalline state changes depending on pH, but it may be related to the rigidity of the distal helix and the stabilities of the salt bridges between the haem propionates and basic HO residues. The binding mode of cyanide to ferric haem–HO should be determined by the energetic balance between the cost of the conformation change of haem–HO seen in the linear binding mode and that of the unusual bent binding of cyanide to the haem iron; at neutral pH, the cost of the conformation change would be increased.

References

Blair-Johnson, M., Fiedler, T. & Fenna, R. (2001). *Biochemistry*, **40**, 13990–13997.

Bolognesi, M., Rosano, C., Losso, R., Borassi, A., Rizzi, M., Wittenberg, J. B., Boffi, A. & Ascenzi, P. (1999). *Biophys. J.* **77**, 1093–1099.

Brünger, A. T., Adams, P. D., Clore, G. M., DeLano, W. L., Gros, P., Grosse-Kunstleve, R. W., Jiang, J.-S., Kuszewski, J., Nilges, M., Pannu, N. S., Read, R. J., Rice, L. M., Simonson, T. & Warren, G. L. (1998). *Acta Cryst.* D**54**, 905–921.

Evans, S. V., Sishta, B. P., Mauk, A. G. & Brayer, G. D. (1994). *Proc. Natl Acad. Sci. USA*, **91**, 4723–4726.

Fedorov, R., Ghosh, D. K. & Schlichting, I. (2003). *Arch. Biochem. Biophys.* **409**, 25–31.

Nakasako, M., Sawano, M. & Kawamoto, M. (2002). *Rev. Sci. Instrum.* **73**, 1318–1320.

Nardini, M., Tarricone, C., Rizzi, M., Lania, A., Desideri, A., De Sanctis, G., Coletta, M., Petruzzelli, R., Ascenzi, P., Coda, A. & Bolognesi, M. (1995). *J. Mol. Biol.* **247**, 459–465.

Neya, S., Funasaki, N., Sato, T., Igarashi, N. & Tanaka, N. (1993). *J. Biol. Chem.* **268**, 8935–8942.

Otwinowski, Z. & Minor, W. (1997). *Methods Enzymol.* **276**, 307–326.

Sen, U., Dasgupta, J., Choudhury, D., Datta, P., Chakrabarti, A., Chakrabarty, S. B., Chakrabarty, A. & Dattagupta, J. K. (2004). *Biochemistry*, **43**, 12477–12488.

Sjögren, T. & Hajdu, J. (2001). *J. Biol. Chem.* **276**, 29450–29455.

Stec, B. & Phillips, G. N. Jr (2001). *Acta Cryst.* D**57**, 751–754.

Sugishima, M., Omata, Y., Kakuta, Y., Sakamoto, H., Noguchi, M. & Fukuyama, K. (2000). *FEBS Lett.* **471**, 61–66.

Sugishima, M., Sakamoto, H., Noguchi, M. & Fukuyama, K. (2003). *Biochemistry*, **42**, 9898–9905.

Sugishima, M., Sakamoto, H., Noguchi, M. & Fukuyama, K. (2004). *J. Mol. Biol.* **341**, 7–13.

Tenhunen, R., Marver, H. S. & Schmid, R. (1968). *Proc. Natl Acad. Sci. USA*, **61**, 748–755.